CHAPTER IV

RESULTS AND DISCUSSION

4.1 Plasma-polymerized polypyrrole films

In general, fabricated undoped polypyrrole films by AC plasma polymerization were obtained as light-brown to black films on the glass slide substrates (**Figure 4.1**). It was found that the color of the films became more intense in color when an increasing power and polymerization time were employed. During optimization to determine appropriate range of AC voltage, it was found that voltage between 800-1500 V was suitable. Therefore, samples were produced at 800, 900, 1000, 1100, 1300, and 1500 V in all cases.

Preliminary investigation showed that a great deal of heat was generated when prolonged reaction time was used. It was cautioned that this may lead to decomposition of film already deposited. Furthermore, it was envisaged that a lifetime of the reactor could be shortened. Therefore, reaction time of 30, 60, and 90 minutes were used. These time period were proven to be optimal since an adequate amount of good quality material was afforded for characterization.

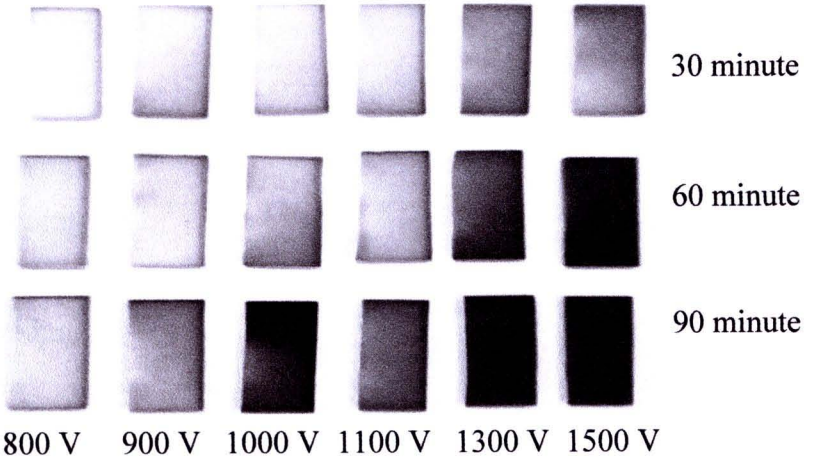

Figure 4.1 Example of plasma-polymerized polypyrrole films by AC plasma polymerization.

4.1.1 Characterization of plasma-polymerized polypyrrole

4.1.1.1 Functional groups and chemical characteristics

ATR-FTIR spectroscopic analysis revealed characteristic peaks of functional groups involved was performed on the AC plasma-polymerized polypyrrole films in order to determine important functional groups present in the material. Representative spectra obtained from films grown at 800, 900, 1000, 1100, 1300, and 1500 V for 30 minutes are displayed in **Figure 4.2**, and data are summarized again in **Table 4.1**. The other reaction times are presented in **Appendices B.1 and B.2**.

Table 4.1 ATR FT-IR band assignments of chemically-synthesized polypyrrole and plasma-polymerized polypyrrole.

Assignments	Wavenumber (cm^{-1})		
	Liquid pyrrole monomer	Chemically-synthesized polypyrrole	Plasma-polymerized polypyrrole
N-H stretching	3430	3400	3349
Aromatic C-H stretching	3187, 3093	3145	3200
Aliphatic C-H stretching	2940	2938	2935, 2851
C≡N stretching, and/or –N=C=O stretching	-	2250	2200, 2232
N-H bending and/or aromatic C=C stretching	1640,1550	1633	1625, 1630
Aliphatic C-N stretching and/or aromatic N-H bending	1200, 1079	1210, 1020	-
C-H out of plant bending in $RCH=CH_2$	1000	-	-
C-H out of plant bending in $R_2C=CH_2$	885	-	-
C-H out of plant bending in $R_2C=CHR$	840	-	-

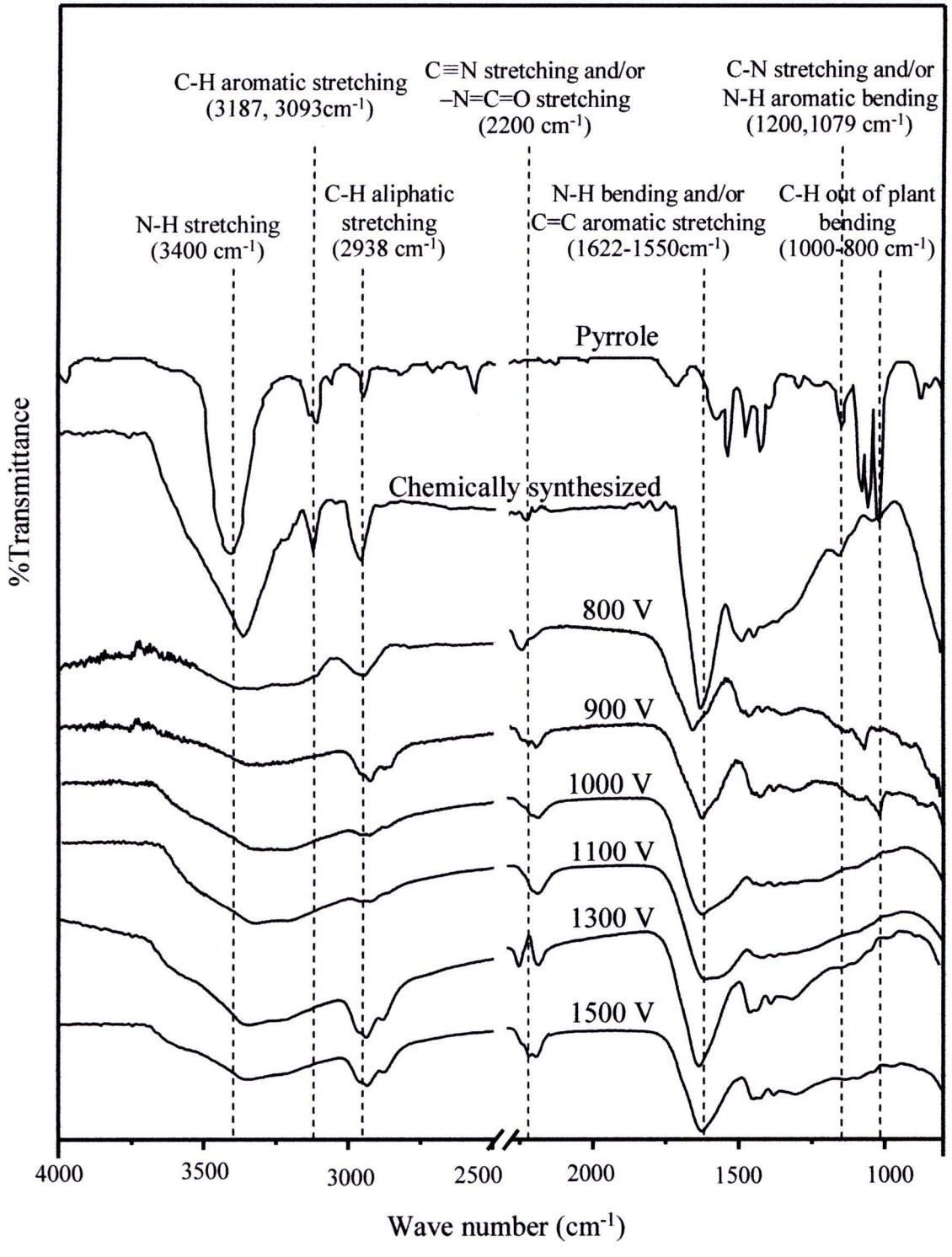

Figure 4.2 FTIR spectrum of liquid pyrrole, and ATR-FTIR spectra of chemically-synthesized, and plasma-polymerized polypyrrole at different AC voltage at 30 minute reaction time.

A spectrum from chemically-synthesized polypyrrole obtained by conventional solution polymerization was also included for comparison. The transmittance spectra of liquid pyrrole, chemically-synthesized polypyrrole, and plasma-polymerized polypyrrole exhibits the following characteristic peaks. Each spectrum includes characteristic peaks of plasma-polymerized polypyrrole found in the case of chemically-synthesized polypyrrole. A band is observed between 3500-3000 cm^{-1}. The bands for a specific absorption can be overlapped in this peak. This peak is assigned to the N-H stretching of the pyrrole ring at 3400 cm^{-1}, while the 3200 cm^{-1} band, associated with the C-H aromatic bonds [14, 19, 26, 31]. However, the absorption of aliphatic C-H bonds is found at 2938 cm^{-1}. This may be resulting from partial fragmentation of the pyrrole ring. The appearance of a peak at 1633 cm^{-1} is due to the N-H bending of amine and/or a C=C aromatic stretching. This peak is strongly suggestive of a conjugated system present in the polypyrrole chain. Alternatively, this can still confirm the existence of the aromatic cyclic structure. The noticeable position at 2200 cm^{-1} maybe assigned to C≡N stretching and/or –N=C=O stretching. From at peak 2200 cm^{-1}, it is found that oxygen contains in the films, but does not consist in liquid pyrrole. This is because oxygen remains in the chamber during polymerization. In the chamber, oxygen and pyrrole conincidentally turn to plasma phase during polymerization with accordance to the result of other authors [29, 34, 36, 56]. The existence of oxygen during polymerization will interfere in polymer chain [33]. Besides, a little oxygen of plasma-polymerized polypyrrole films is in liquid monomer, air, or desiccator. The appearance of a peak at 1200 cm^{-1} is aliphatic C-N stretching and/or N-H aromatic bending. This is not found in plasma-polymerized polypyrrole due to fragmentation of pyrrole ring.

The vibrational frequencies of pyrrole for the plasma polymer and chemically-polypyrrole correspond to frequencies of liquid pyrrole in the region of 1440-1400 cm^{-1}, as shown in **Figure 4.2**. This region is not significant in consideration because of the bands of the in-plane vibration of ring. The other peak in the range of 800-1000 cm^{-1} contains many absorptions corresponding to alkenes from some broken ring and C-H out of plane bending [29, 35, 36]. When comparing IR absorption frequencies between those observed in the spectra chemically-synthesized

polypyrrole and plasma-polymerized polypyrrole, it is exhibited that peaks of both polymers similarly show major absorptions.

In general, observed peaks of the films are broader than that of liquid pyrrole and chemically-synthesized polypyrrole. This is consistent with amorphous structure of the plasma polymerized material. Since numerous different fragments, radicals, ions, *etc.* are generated in the plasma process due to its high energy, a high degree of crosslinking would take place.

4.1.1.2 Elemental composition of the films

Elemental analysis is used to analyze compositions of carbon and nitrogen in films which cannot analyze hydrogen composition. Therefore, in this work, ratio of carbon to nitrogen is presented. Results from the elemental analysis of plasma-polymerized polypyrrole are shown in **Table 4.2,** and raw data are tabulated in **Appendix C.1**. In this study, it was found that the atomic ratio of carbon to nitrogen (C/N) in the chemically-synthesized polypyrrole is calculated to be 4.7/1. The elemental compositions of plasma-polymerized polypyrrole were compared with the value from of chemically-synthesized polypyrrole. In this case, a C/N ratio close to the chemically-synthesized would indicate that the plasma-polymerized polypyrrole was not much damage.

Table 4.2 The AC voltages versus C/N ratio of plasma-polymerized polypyrrole.

AC voltages (V)	The atomic ratio of C/N		
	30 minute	60 minute	90 minute
800	4.0	4.3	4.8
900	4.4	4.7	4.9
1000	4.3	5.0	5.6
1100	5.4	5.2	5.9
1300	4.1	5.7	4.5
1500	4.0	4.2	4.8

However, from data in **Table 4.1**, it can be clearly seen that most plasma-polymerized polypyrrole films have a C/N ratio from 4.0 to 5.9 which

corresponds to chemically-synthesized polypyrrole (4.7). Therefore, from the C/N ratio, the structure of plasma-polymerized pyrrole should be similar to chemically-synthesized. In ideal polypyrrole, the C/N ratio is at 4.0 which corresponds to the ratio of plasma-polymerized polypyrrole at voltages of 800, 1300, and, 1500 V for 30 minute. But at voltages of 900, 1000, 1100, and 1500 V, the C/N ratio of plasma-polymerized pyrrole films is higher than the ideal C/N ratio of polypyrrole. According to IR spectra, the spectrum of chemically-synthesized polypyrrole differs from those of plasma-polymerized polypyrrole films. For chemically-synthesized polypyrrole, a sharp peak occurs at 3400 cm^{-1} and another peak is at 3093 cm^{-1}. In this range, plasma-polymerized polypyrrole films yields a band between 3500 and 3000 cm^{-1}. This band will overlap in these peaks of chemically-synthesized polypyrrole. This means that pyrrole ring is broken during plasma polymerization, as seen in **Figure 4.3** showing a structure model of plasma-polymerized polypyrrole estimated from ATR-FTIR spectra and EDS analysis data [19, 25].

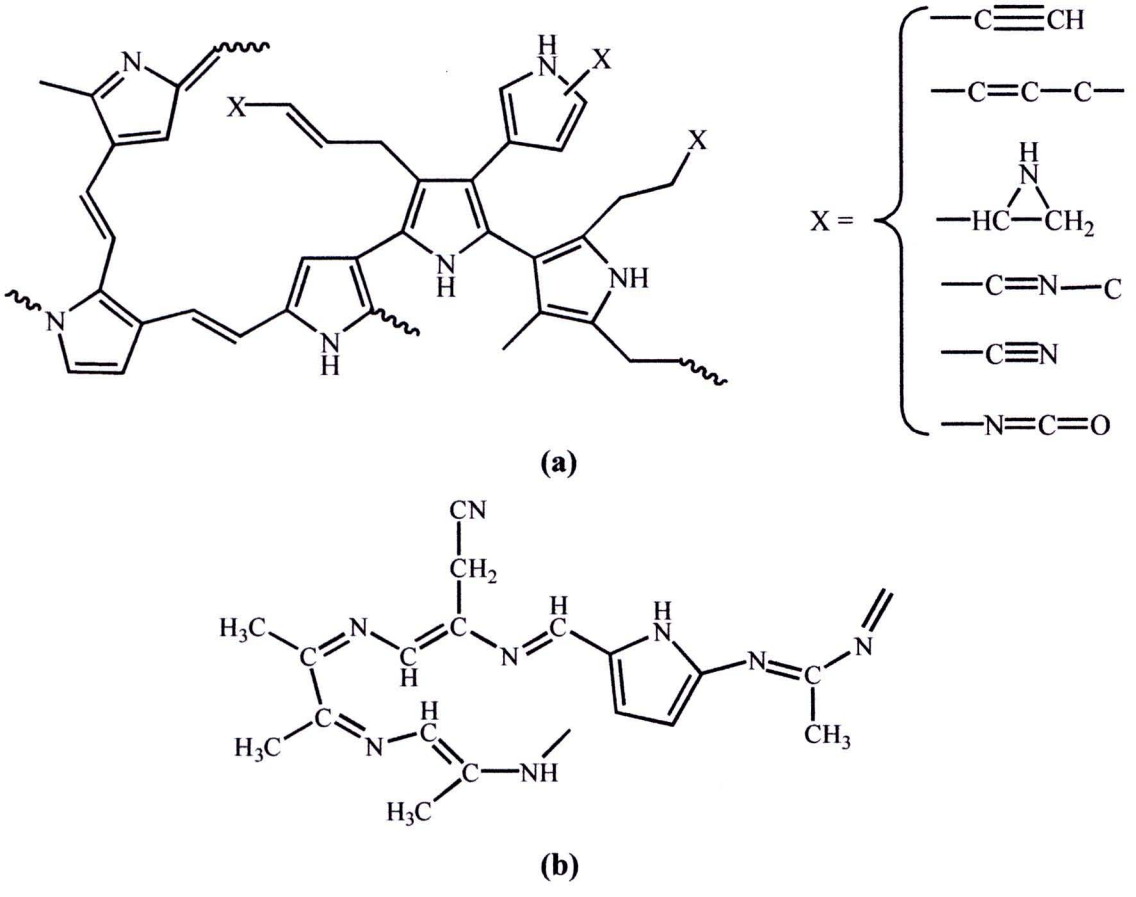

Figure 4.3 Proposed structures of plasma-polymerized polypyrrole [19, 25].

Energy bonds of C-C, C=C, and C-N are 348, 614, and 305 kJ mol^{-1}, respectively, and then the effect of plasma polymerization maybe has C-C and C-N bonds broken. Furthermore, the increase in electron density may result in an increase in the number of collisions between electrons and other plasma species [63]. Therefore, from IR and EDS results, it confirms that the characteristics of the pyrrole rings remain in the plasma-polymerized polypyrrole film.

4.1.1.3 Film morphology

The morphology of plasma-polymerized polypyrrole films was observed by SEM analysis. SEM displayed in **Figure 4.4**, **4.5**, and **4.6** indicated that the polypyrrole films became smooth at the voltage less than 1100 V. When the voltage is higher than 1100 V, the surface is found that there are grains appearing in it. At the low discharge, the disposition rate is low; therefore, the polymer chain has more time to arrange the structure on the surface. This leads to the film showing smooth surface. The deposition rate is increased with applied voltage as shown in **Table 4.3**. The thickness of plasma-polymerized polypyrrole films is significantly affected by AC voltage and reaction time. In addition, SEM cross-section displayed that plasma-polymerized polypyrrole have dense and pinhole-free films all applied voltages as shown in **Figure 4.7**.

Table 4.3 The film thickness at various AC voltages and reaction times.

AC voltages (V)	Thickness (μm)		
	30 minute	60 minute	90 minute
800	0.32	1.09	1.93
900	0.87	1.71	1.99
1000	1.42	2.05	3.36
1100	1.60	2.66	4.18
1300	2.02	3.04	4.84
1500	2.65	3.38	5.75

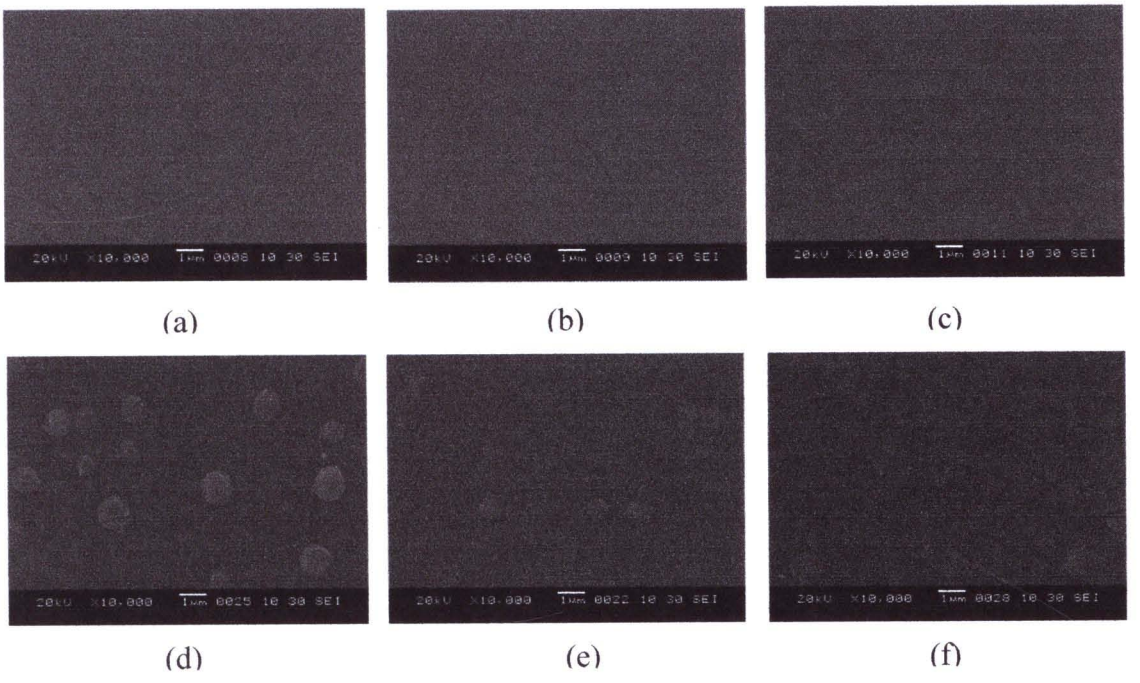

(a) (b) (c)

(d) (e) (f)

Figure 4.4 Morphology of plasma-polymerized polypyrrole films on the glass substrate determined by scanning electron microscopic technique at 30 minute and various voltages; (a) 800 V, (b) 900 V, (c) 1000 V, (d) 1100 V, (e) 1300 V, and (f) 1500 V.

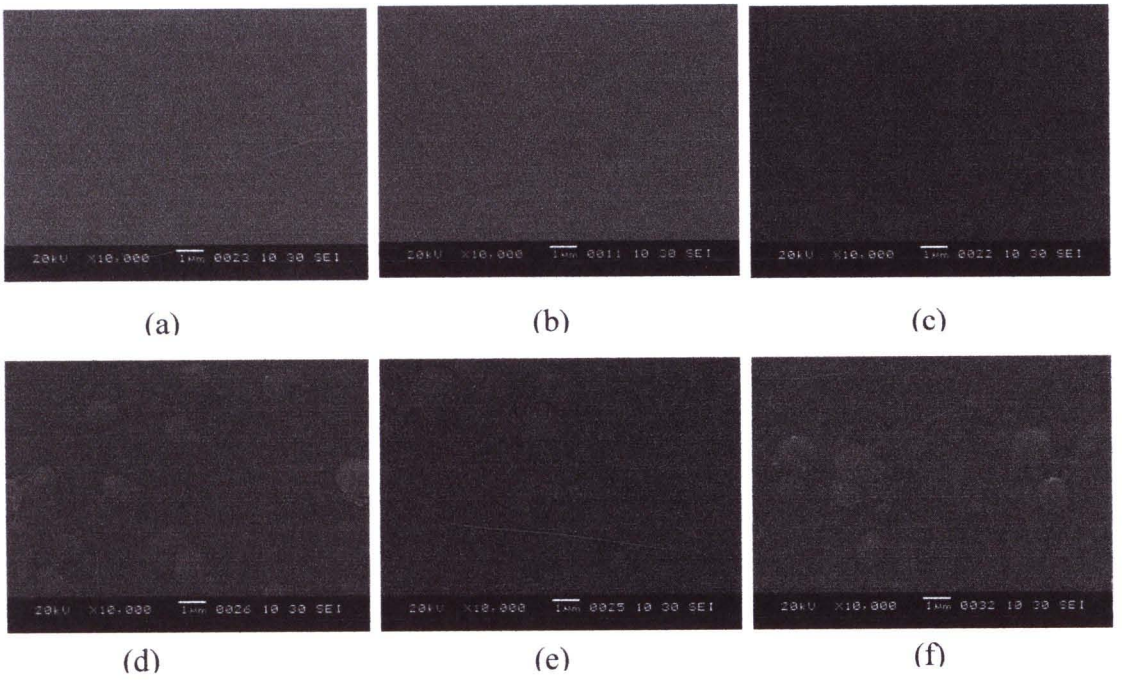

(a) (b) (c)

(d) (e) (f)

Figure 4.5 Morphology of plasma-polymerized polypyrrole films on the glass substrate determined by scanning electron microscopic technique at 60 minute and various voltages; (a) 800 V, (b) 900 V, (c) 1000 V, (d) 1100 V, (e) 1300 V, and (f) 1500 V.

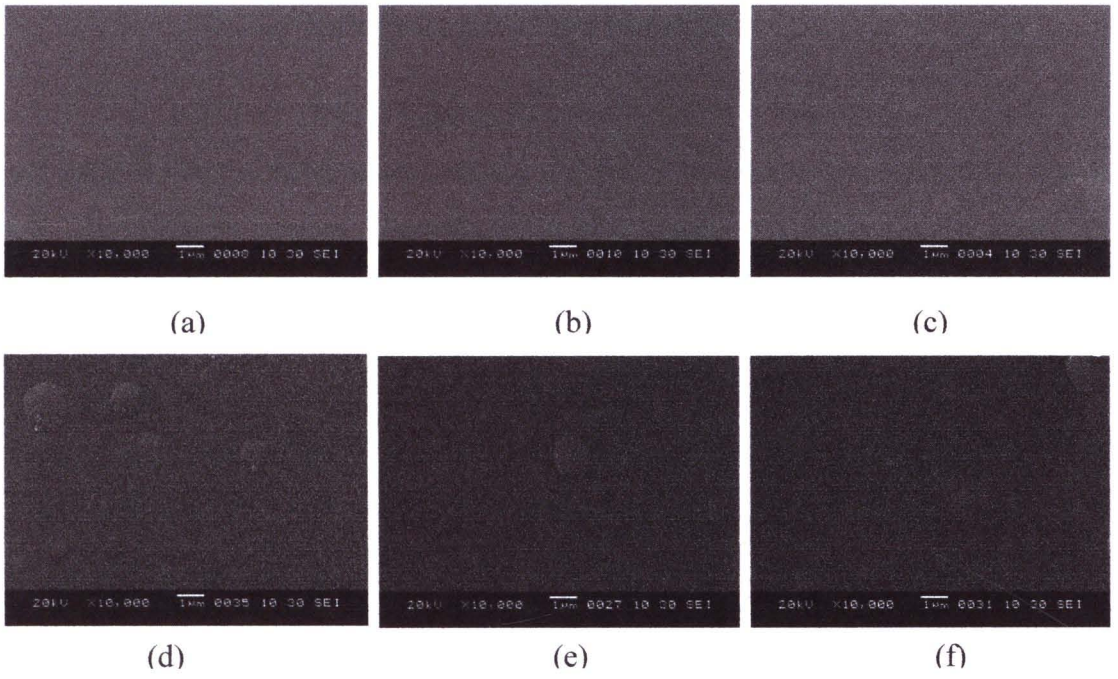

Figure 4.6 Morphology of plasma-polymerized polypyrrole films on the glass substrate determined by scanning electron microscopic technique at 90 minute and various voltages; (a) 800 V, (b) 900 V, (c) 1000 V, (d) 1100 V, (e) 1300 V, and (f) 1500 V.

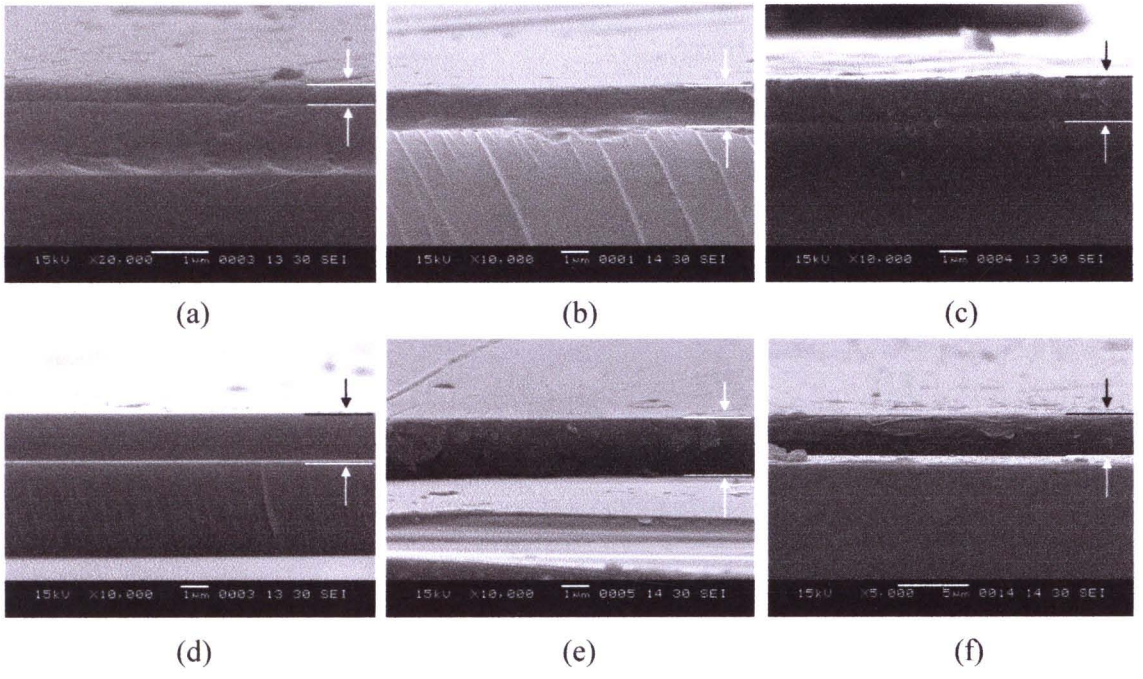

Figure 4.7 Cross-sectional analysis of plasma-polymerized polypyrrole films on the glass substrate determined by scanning electron microscopic technique at 30 min and various voltages; (a) 800 V, (b) 900 V, (c) 1000 V, (d) 1100 V, (e) 1300 V, and (f) 1500 V.

4.1.1.4 Optical characteristics of the films

The UV-Vis maximum absorption of the plasma-polymerized polypyrrole films at different AC voltage and reaction times are summarized in **Table 4.4**. The UV-Vis spectra illustrated that the absorption maxima of polypyrrole fabricated by plasma polymerization at 30 minute (**Figure 4.8**), 60 minute (**Figure 4.9**), and 90 minute (**Figure 4.10**) assigned to the π-π^* transition were noticed at around 356-370 nm, 342-365 nm, and 328-360 nm, respectively.

From **Table 4.4**, it has been shown that as the AC voltage decreased; absorption was observed at relatively longer wavelength. This is suggestive of a longer π-electron conjugation length in the plasma-polymerized polypyrrole films which resulted in a red shift with an increase in the AC voltage used. The highest wavelength was observed at the voltage of 800 V for 30 minute. It is expected that electrical conductivity of this condition higher than other condition.

Table 4.4 The conclusion of UV-Vis maximum absorption (λ_{max}) of plasma-polymerized polypyrrole.

AC voltages (V)	λ_{max} (nm)		
	30 minute	60 minute	90 minute
800	370	365	358
900	365	360	360
1000	354	347	344
1100	359	342	344
1300	358	350	338
1500	356	345	326

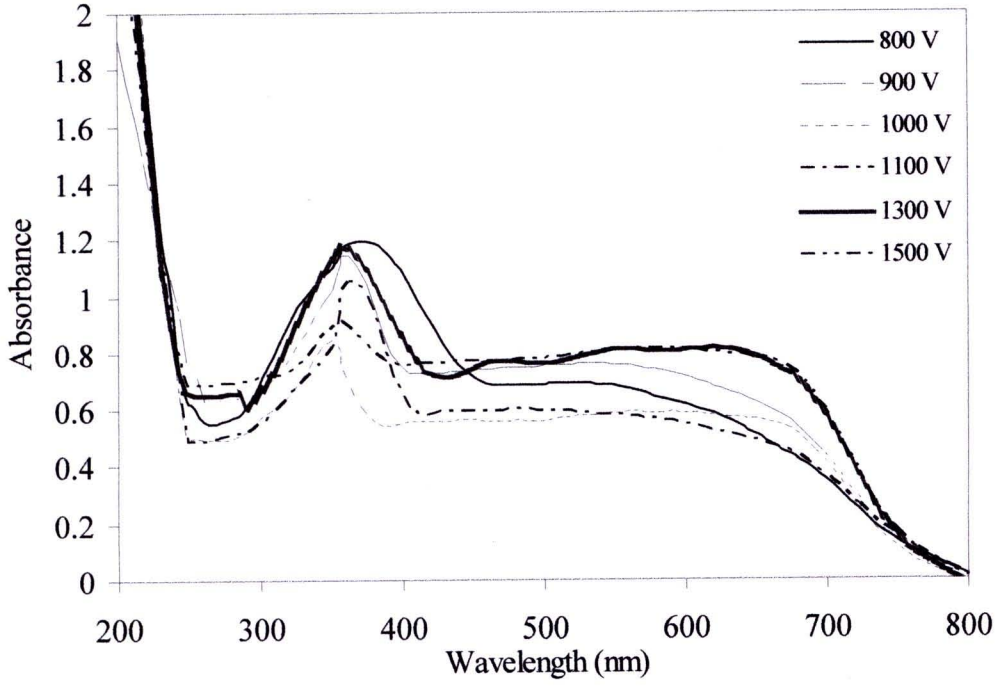

Figure 4.8 UV-Vis absorbance spectra of plasma-polymerized polypyrrole at different AC voltage at 30 minute reaction time.

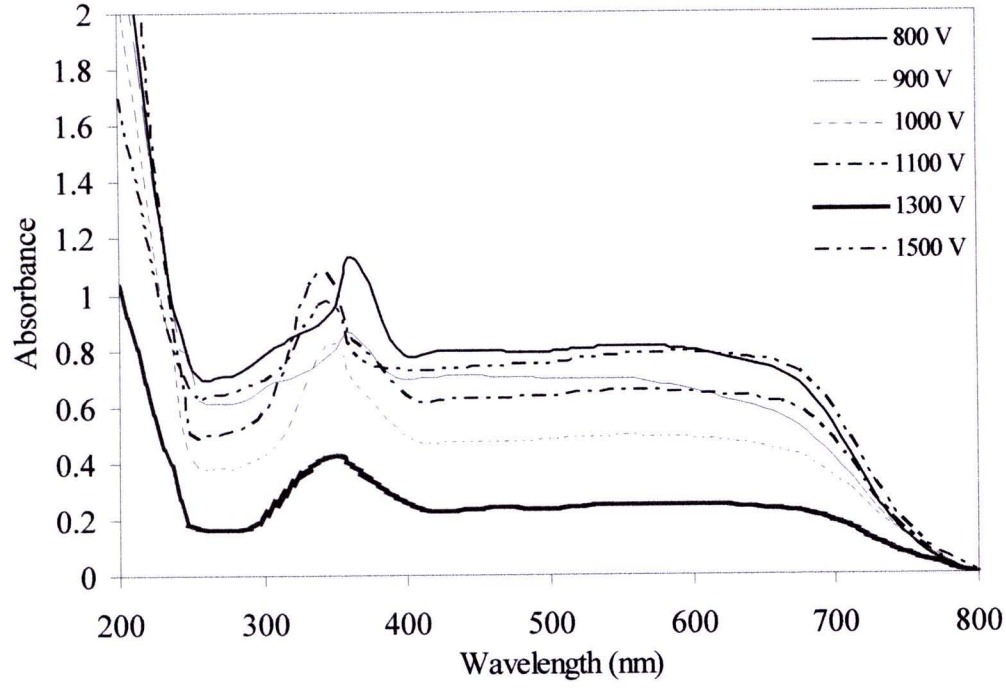

Figure 4.9 UV-Vis absorbance spectra of plasma-polymerized polypyrrole at different AC voltage at 60 minute reaction time.

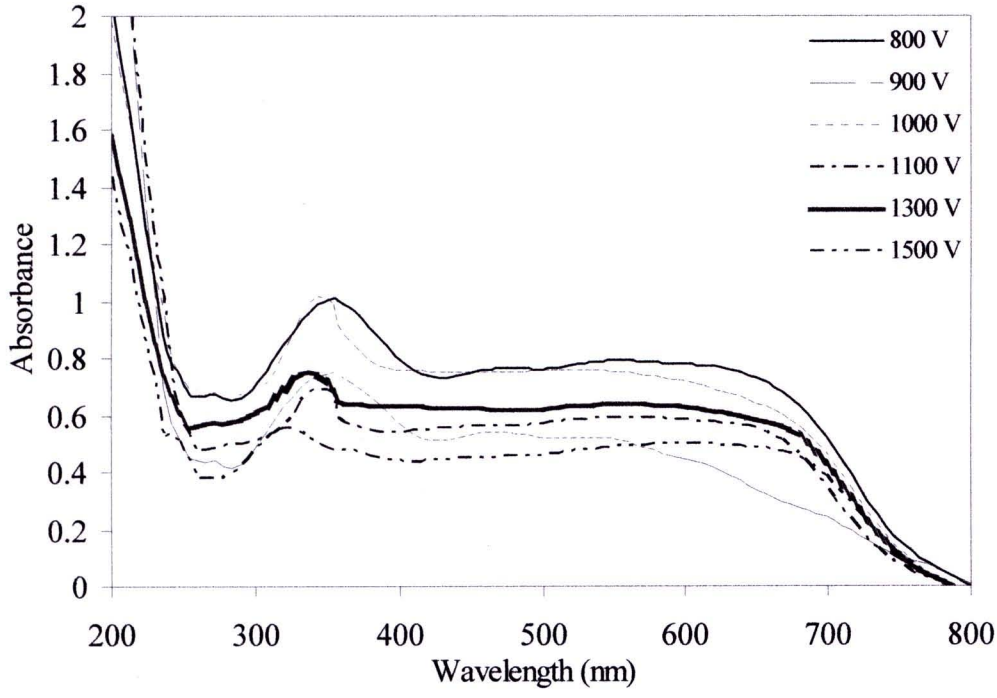

Figure 4.10 UV-Vis absorbance spectra of plasma-polymerized polypyrrole at different AC voltage at 90 minute reaction time.

4.1.1.5 Electrical conductivity

The conductivity of the polypyrrole films deposited on glass substrates were measured using a two-probe method. In general, the electrical conductivity of the *I-V* characteristics was measured between 0-100 V. The typical plot for current versus voltage is depicted in **Figure 4.11**. In this study *I-V* characteristic shows linearity which complies with Ohmic's law [64].

Table 4.5 summarized conductivity of the fabricated films at various AC voltages at 30, 60, and 90 minutes. The conductivity of AC plasma-polymerized polypyrrole films is in the range of 3.4×10^{-8} – 67.2×10^{-8} S/cm. It was observed the decrease of the conductivity increases with the reaction time and AC voltage in correspondence with the result of UV-Vis spectroscopy.

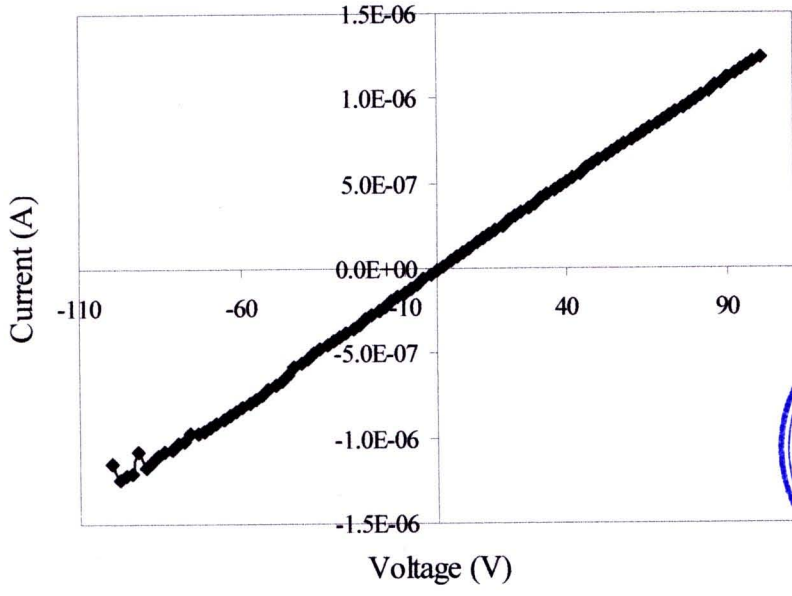

Figure 4.11 The plot of current versus voltage at room temperature.

Table 4.5 The electrical conductivity of AC plasma-polymerized polypyrrole.

AC voltages (V)	Conductivity (S/cm)		
	30 minute	60 minute	90 minute
800	67.2×10^{-8}	18.8×10^{-8}	9.5×10^{-8}
900	20.7×10^{-8}	10.8×10^{-8}	10.4×10^{-8}
1000	6.1×10^{-8}	6.2×10^{-8}	4.2×10^{-8}
1100	8.3×10^{-8}	5.5×10^{-8}	3.9×10^{-8}
1300	10.3×10^{-8}	7.5×10^{-8}	4.3×10^{-8}
1500	8.4×10^{-8}	6.1×10^{-8}	3.4×10^{-8}

4.2 *In situ* iodine-doped plasma-polymerized polypyrrole films

4.2.1 Characterization of *in situ* iodine-doped plasma-polymerized polypyrrole

4.2.1.1 Functional groups and chemical characteristics

The ATR-FTIR spectra of *in situ* iodine-doped plasma-polymerized polypyrrole by AC plasma polymerization at different AC voltages for 30 minute are shown in **Figure 4.12**. The other reaction times are presented in **Appendices B.3 and**

B.4. As mentioned earlier that in the plasma process numerous different fragments, for instance radicals, ions, *etc.* could be generated, therefore complex chemical structures of plasma-polymerized polypyrrole are not totally unforeseen. Moreover, many reactions with iodine may occur during the *in situ* doping process. This may also result in an even more amorphous structure of the films. Consequently, the ATR-FTIR spectra are broad.

Figure 4.12 represents the IR spectra of pyrrole monomers and plasma-polymerized polypyrrole films prepared in the absence (800 V) and in the presence of iodine at various AC voltages for 30 minute. A comparison of the eight spectra revealed that a board peak due to N-H stretching was present at 3500-3000 cm^{-1} and the absorption peak at 1622-1550 cm^{-1} correspond to C=C stretching was showed in all of the spectra.

For *in situ* iodine-doped plasma-polymerized polypyrrole, the new absorption band appears at 1120 cm^{-1} and has been assigned as a C-H out of plane bending [65]. Another peak around 1400 cm^{-1}, might be assigned to the $-CH_2I$ and/or $-CI=CH_2$ stretching [29, 66]. Those peaks are importance due to its show iodine impact in the plasma-polymerized polypyrrole film.

In the plasma process, numerous different fragments, for instance radicals, ions, *etc.* could be generated. Therefore, complex chemical structures of plasma-polymerized polypyrrole are not totally unforeseen. Moreover, many reactions with iodine may occur during the *in situ* doping process. Iodine probably reacted with residual radicals in the plasma-polymerized pyrrole films. In addition, iodine radicals may be able to remove hydrogen atoms from pyrrole structures because the aromatic structure can stabilize the resulting radical [66]. The radical on the pyrrole structure can in its turn react with other iodine radicals to form mono-substituted pyrrole as shown in Eq. 4.1-4.4.

$$I_2 \leftrightarrow 2I^{\bullet} \qquad 4.1$$

$$PPy + I^{\bullet} \rightarrow PPy^{\bullet} + HI \qquad 4.2$$

$$PPy^{\bullet} + I_2 \rightarrow PPyI + I^{\bullet} \qquad 4.3$$

$$2HI \rightarrow H_2 + I_2 \qquad 4.4$$

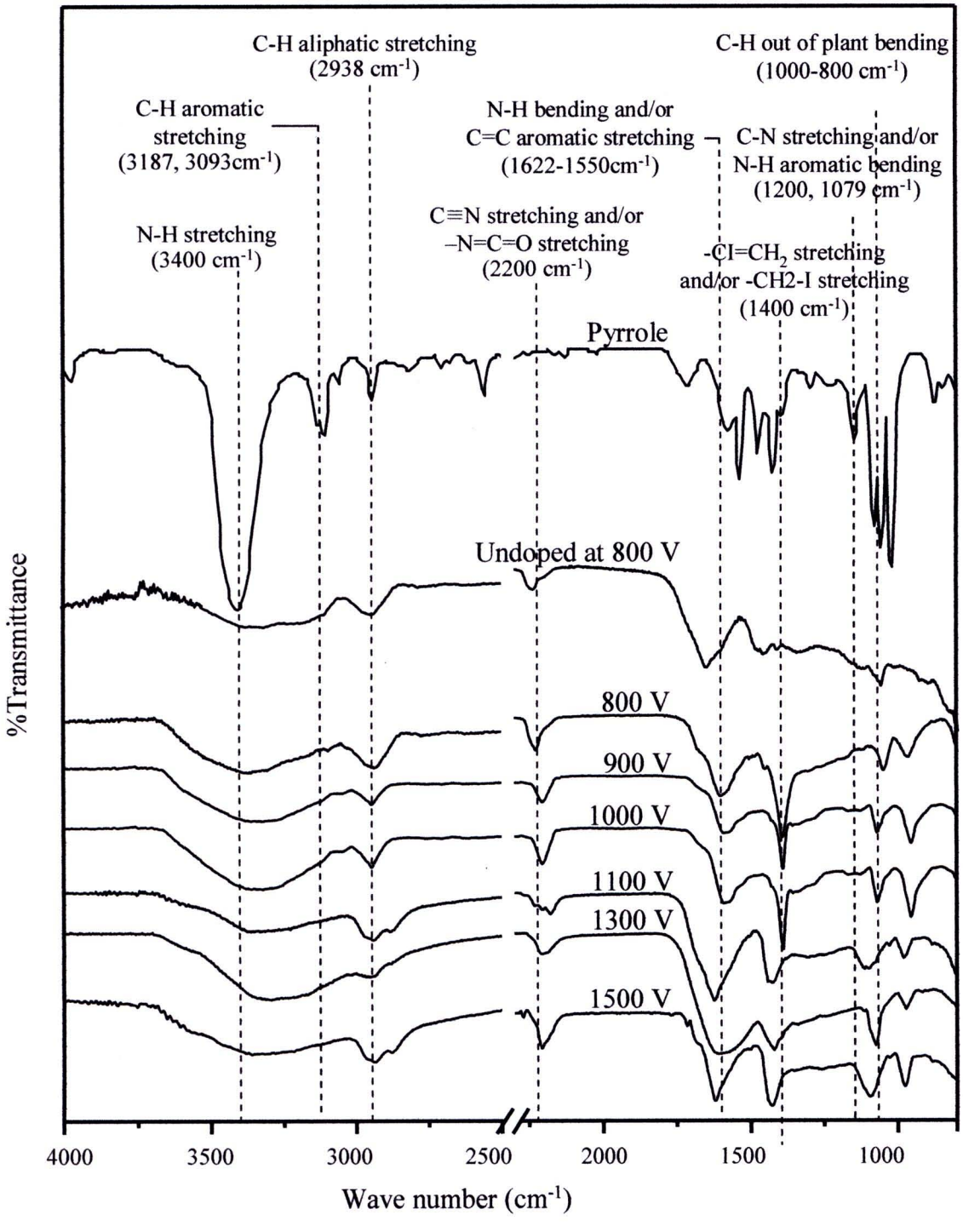

Figure 4.12 FTIR spectrum of liquid pyrrole, and ATR-FTIR spectra of undoped at 800 V for 30 minute and *in situ* iodine-doped plasma-polymerized polypyrrole at different AC voltages at 30 minute reaction time.

4.2.1.2 Elemental composition of the films

EDS characterization verified the presence of iodine in the *in situ* iodine-doped films. The atomic ratio of iodine to nitrogen (I/N) and carbon to nitrogen (C/N) of *in situ* iodine-doped plasma-polymerized polypyrrole films in ranged to 0.2-3.2 and.5.2-8.2, respectively, as shown in **Table 4.6** and raw data presented in **Appendix C.2**. From **Table 4.6** shown the I/N of these polypyrrole films was decreased with increased voltage.

Table 4.6 The AC voltages versus C/N ratio (a) and I/N ratio (b) of *in situ* iodine-doped plasma-polymerized polypyrrole.

AC	The atomic ratio of C/N			The atomic ratio of I/N		
voltages (V)	30 minute	60 minute	90 minute	30 minute	60 minute	90 minute
800	6.2	7.5	6.9	2.7	2.7	3.0
900	6.8	6.9	7.2	1.8	2.2	3.2
1000	7.1	8.0	8.2	2.9	3.1	2.5
1100	5.8	6.4	6.1	1.3	2.0	1.7
1300	7.3	6.3	5.2	1.4	1.1	1.2
1500	5.5	6.8	5.5	0.3	1.0	1.2

It was proposed by Groenewoud [66] that when the iodine vapor suffers the plasma, iodine molecule is broken to iodine radical. An iodine radical can then capture an electron from plasma environment resulting in the formation of monoiodine ion (I^-). Even with the detection of the I^- ion, it was found that I_3^- and I_5^- are the most important forms.

$$I_2 \rightarrow 2I^{\bullet}$$
$$I^{\bullet} + \bar{e} \rightarrow I^-$$
$$I^- + I_2 \rightarrow I_3^-$$
$$I_3^- + I_2 \rightarrow I_5^-$$

From ATR-FTIR spectra and EDS, it is possible that a small degree of the pyrrole ring might have been decomposed to some extension in the plasma-

polymerized polypyrrole films. This may have resulted in the loss of a small amount of nitrogen atoms from the rings. This is consistent with the finding by Hosono [19, 26, 27] that some pyrrole rings of the plasma-polymerized polypyrrole were decomposed to form a three-dimensional network. Nevertheless, the ATR-FTIR and the EDS results, still confirms that the characteristics of the pyrrole rings are largely preserved in the plasma-polymerized polypyrrole film. Higher C/N elemental compositions were found in the case of *in situ* iodine-doped plasma-polymerized polypyrrole compared those of undoped plasma-polymerized polypyrrole. It is proposed that the increase is a result of an impact of a large iodine atom on some of the pyrrole rings in the gas phase during polymerization. As a consequence, loss of nitrogen might occur at higher degree which gave rise to higher C/N ratios.

4.2.1.3 Film morphology

The *in situ* iodine-doped plasma-polymerized polypyrrole films by AC plasma polymerization were almost identical to that of films compared to those of the undoped polypyrrole films. *In situ* iodine-doped polypyrrole films were found to be in the range of 0.64 to 5.19 μm (**Table 4.7**) thickness as determined by SEM analysis. The effects of AC voltages and reaction times on the morphology are shown in **Figure 4.13**, **Figure 4.14**, and **Figure 4.15** for 30, 60, and 90 minute, respectively. At higher AC voltage and longer reaction time was exhibit increasingly a size of grain on the surface. This may be attributed to be the result of iodine impact upon the polymer chains.

Table 4.7 The film thickness of *in situ* iodine-doped plasma-polymerized polypyrrole at various AC voltages and reaction times.

AC voltages (V)	Thickness (μm)		
	30 minute	60 minute	90 minute
800	0.64	0.82	1.24
900	0.72	1.42	1.86
1000	1.50	1.92	3.32
1100	1.60	2.56	4.08
1300	1.90	3.02	4.76
1500	2.26	3.24	5.19

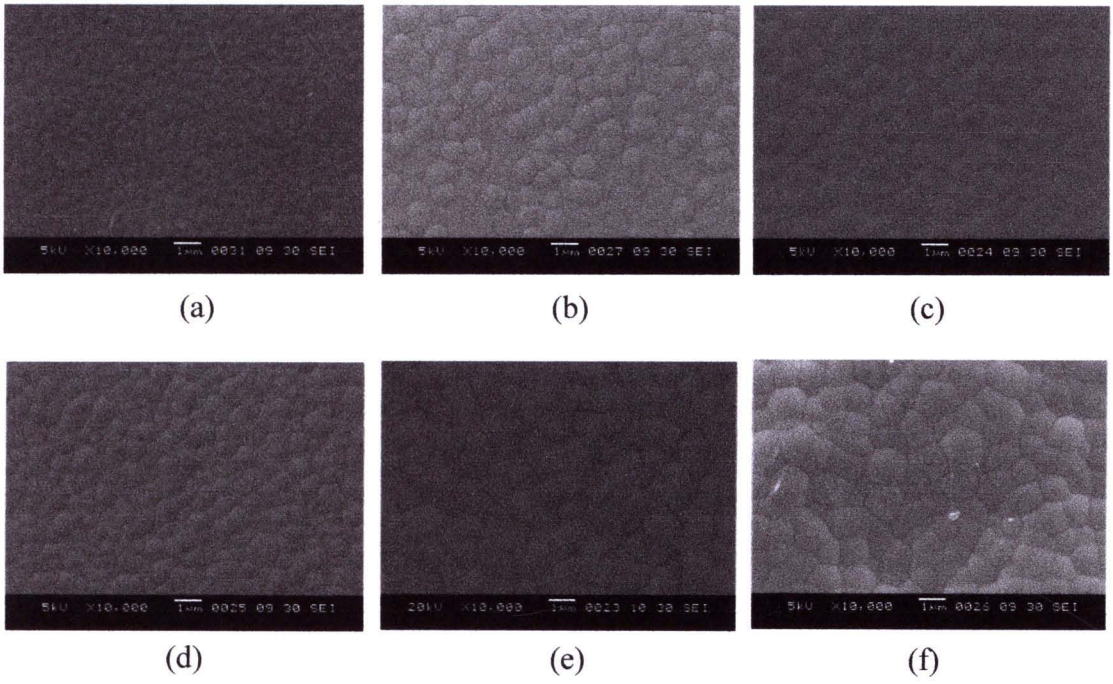

(a) (b) (c)

(d) (e) (f)

Figure 4.13 Morphology of *in situ* iodine-doped plasma-polymerized polypyrrole films on the glass substrate determined by scanning electron microscopic technique at 30 minute and various voltages; (a) 800 V, (b) 900 V, (c) 1000 V, (d) 1100 V, (e) 1300 V, and (f) 1500 V.

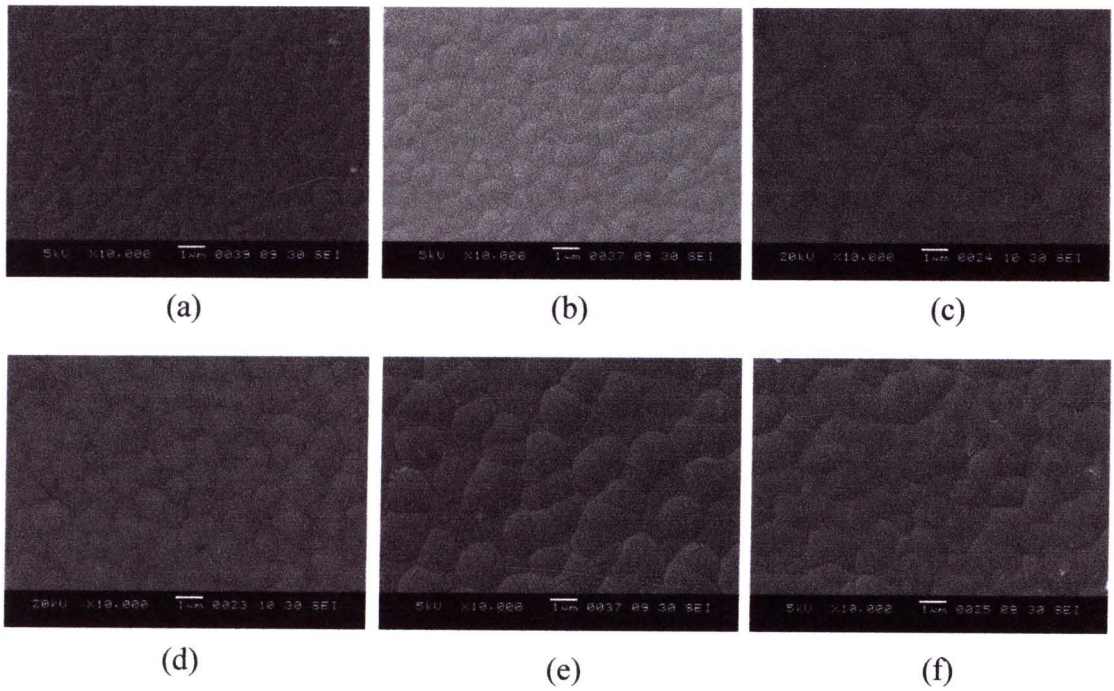

(a) (b) (c)

(d) (e) (f)

Figure 4.14 Morphology of *in situ* iodine-doped plasma-polymerized polypyrrole films on the glass substrate determined by scanning electron microscopic technique at 60 minute and various voltages; (a) 800 V, (b) 900 V, (c) 1000 V, (d) 1100 V, (e) 1300 V, and (f) 1500 V.

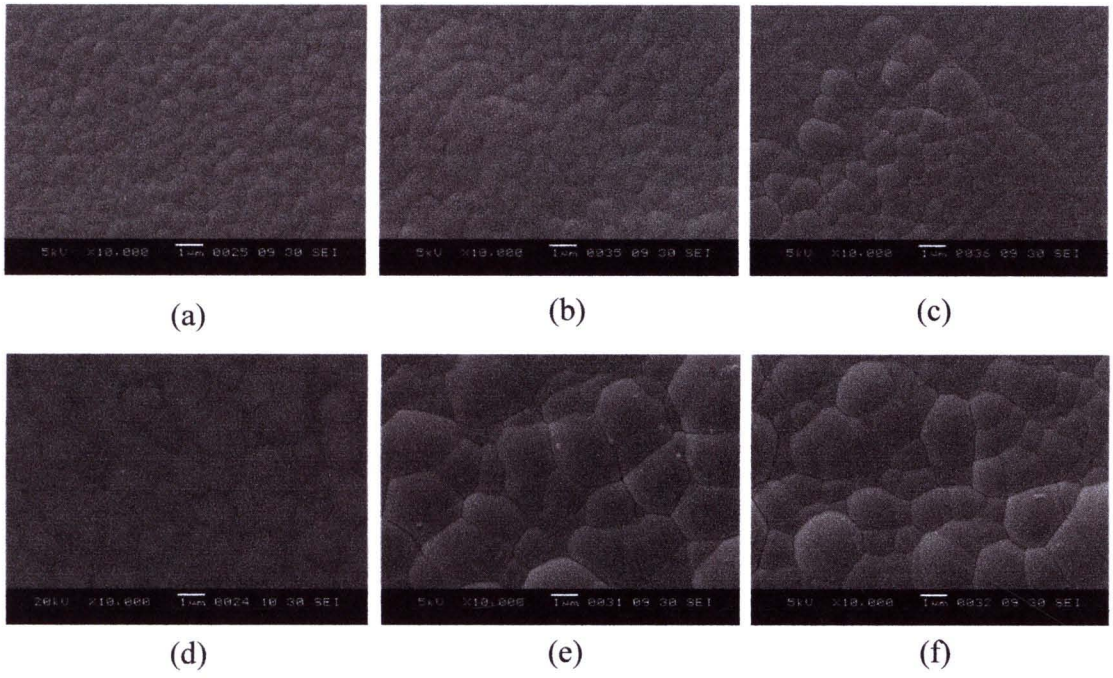

Figure 4.15 Morphology of *in situ* iodine-doped plasma-polymerized polypyrrole films on the glass substrate determined by scanning electron microscopic technique at 90 minute and various voltages; (a) 800 V, (b) 900 V, (c) 1000 V, (d) 1100 V, (e) 1300 V, and (f) 1500 V.

4.2.1.4 Optical characteristics of the films

The *in situ* iodine-doped plasma-polymerized polypyrrole films by AC plasma polymerization gave products that showed the absorption maxima around 385 to 431 nm as shown in **Figure 4.16**, **Figure 4.17**, and **Figure 4.18** and summarized in **Table 4.8** which shift to higher wavelength than those of undoped polypyrrole (326 to 370 nm) were evident. From **Table 4.8**, it has been shown here that as the AC voltage decreased; absorption was observed at relatively longer wavelength similar undoped films. This confirms the incorporation of iodine in the films. The shift of UV absorption is strongly suggestive of the formation of the $(PPy)^{+}I^{-}$ charge-transfer complex. Consequently, an enhanced electrical conductivity was also observed. The highest wavelength was observed at the voltage of 800 V for 30 minute. It is expected that electrical conductivity of this condition higher than other condition.

Table 4.8 The summation of UV-Vis maximum absorption (λ_{max}) of *in situ* iodine-doped plasma-polymerized polypyrrole.

AC voltages (V)	λ_{max} (nm)		
	30 minute	60 minute	90 minute
800	431	414	412
900	425	410	400
1000	409	403	397
1100	403	400	391
1300	400	397	390
1500	398	391	385

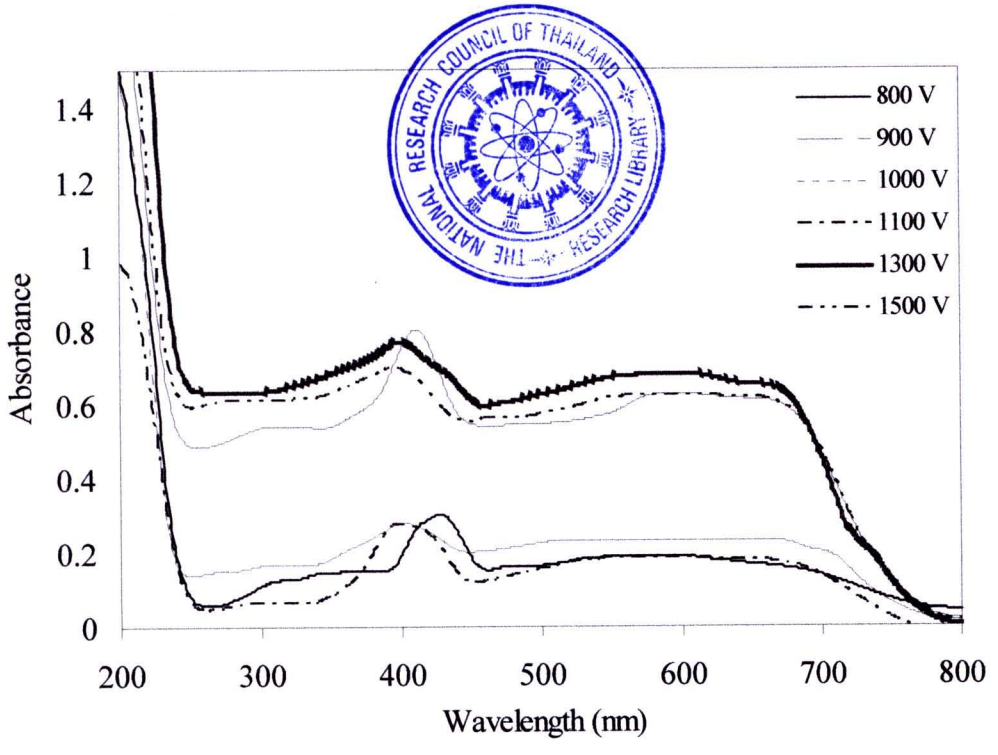

Figure 4.16 UV-Vis spectra of *in situ* iodine-doped plasma-polymerized polypyrrole at 30 minute and various voltages.

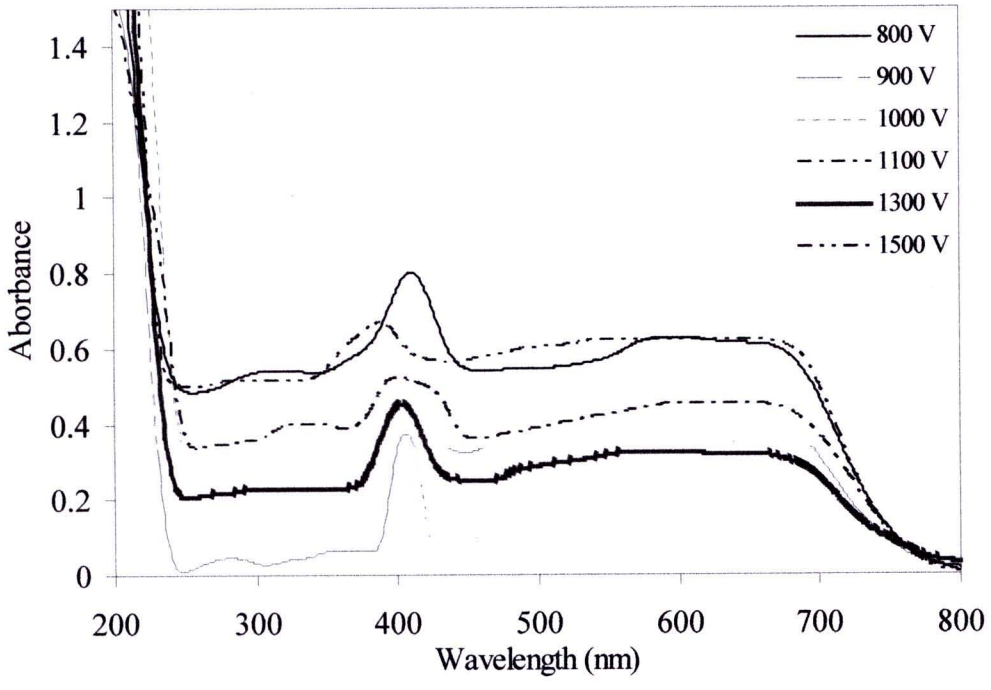

Figure 4.17 UV-Vis spectra of *in situ* iodine-doped plasma-polymerized polypyrrole at 60 minute and various voltages.

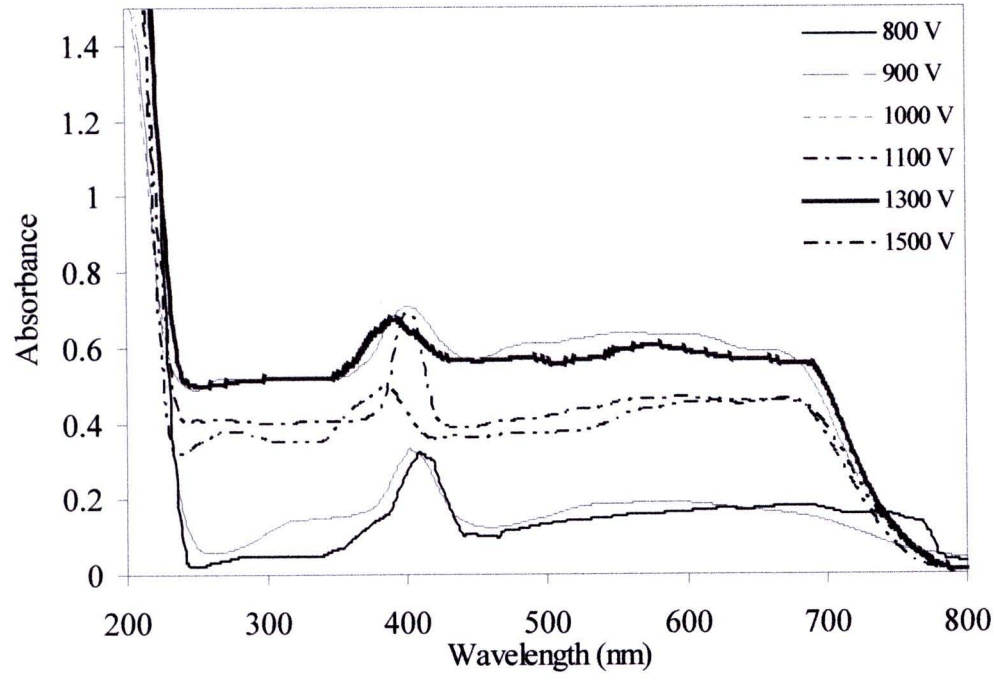

Figure 4.18 UV-Vis spectra of *in situ* iodine-doped plasma-polymerized polypyrrole at 90 minute and various voltages.

4.2.1.5 Electrical conductivity

The conductivity of *in situ* iodine-doped plasma-polymerized polypyrrole films are summarized in **Table 4.9**. This shown at higher AC voltage and longer reaction time was exhibit decreasingly electrical conductivity of iodine-doped films. These results were consistent with undoped plasma-polymerized polypyrrole films.

Table 4.9 The electrical conductivity of *in situ* iodine-doped plasma-polymerized polypyrrole films.

AC voltages (V)	Conductivity (S/cm)		
	30 minute	60 minute	90 minute
800	16.6×10^{-7}	12.5×10^{-7}	8.4×10^{-7}
900	14.2×10^{-7}	6.8×10^{-7}	5.4×10^{-7}
1000	4.7×10^{-7}	3.7×10^{-7}	2.2×10^{-7}
1100	4.9×10^{-7}	3.8×10^{-7}	2.4×10^{-7}
1300	4.8×10^{-7}	3.2×10^{-7}	2.0×10^{-7}
1500	4.4×10^{-7}	3.1×10^{-7}	1.9×10^{-7}

It is evident that the measured values (1.9×10^{-7} to 16.6×10^{-7} S/cm) are upto one orders of magnitude higher than the usual range of conductivity of undoped plasma-polymerized polypyrrole (3.4×10^{-8} to 67.2×10^{-8} S/cm) as shown in **Figure 4.19**. This result indicated that the *in situ* doping can indeed enhance the electrical conductivity of the films. For comparison purposes, reported electrical conductivity values of iodine-doped conventional chemically-synthesized, electrochemically-synthesized polypyrrole and other plasma-polymerized polypyrrole are tabulated and shown in **Table 4.10**.

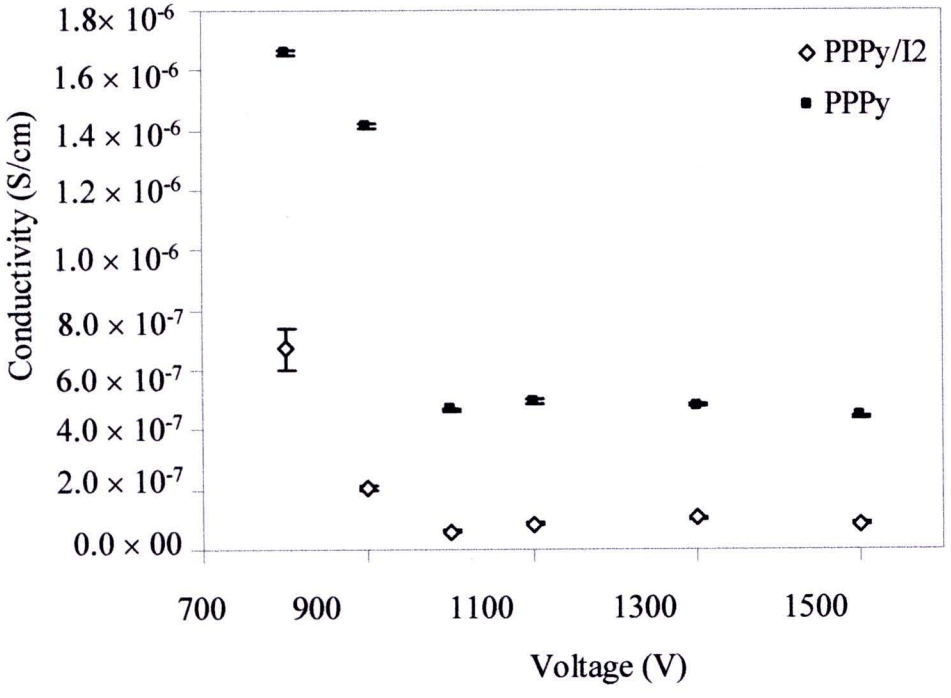

Figure 4.19 The conductivity of undoped and *in situ* iodine-doped plasma-polymerized polypyrrole at 30 minute and various voltages.

Table 4.10 Compare the electrical conductivity of iodine-doped polypyrrole by conventional and different plasma polymerization method.

Entry	Polymerization method [Ref]	Doping method (Doping period)	Conductivity (S/cm)
1	Chemical [29]	*ex situ* doping (unspecified)	2.0×10^{-7}
2	Electrochemical [67]	*ex situ* doping (unspecified)	0.5×10^{-7}
3	RF-plasma [29]	*ex situ* doping, 20 minute	0.1×10^{-7}
4	RF-plasma [14]	*in situ* doping, 60 minute	10.0×10^{-7}
5	Pulsed RF plasma [28]	*ex situ* doping, 300 minute	0.01×10^{-7}
6	AC plasma	*in situ* doping, 30 minute	16.6×10^{-7}
7	AC plasma	*ex situ* doping, 24 hours	32.0×10^{-7}

Note: RF = Radio frequency

From the literature reports, most of the doping processes were carried out after the synthesis of the films by exposing the films to an iodine vapor in a sealed container at various lengths of time [29]. In the case of entry 4 [14], there was the *in situ* doping carried out. By this means of doping, the dopant element iodine was

introduced directly with the monomer into the plasma process. It is obvious that the conductivity of the *ex situ* doping films lower *in situ* doping films. In general it can been seen that in the case of conventional electrochemical as well as chemically-polymerized film, after being doped initial electrical conductivity were exhibited. However, over a period of time, conductivities were reported to decrease to more or less a value of an undoped material.

In the case conventional chemically-polymerized and electrochemical film can been seen that after being doped initial electrical conductivity were exhibited. However, over a period of time, conductivities were reported to decrease to more or less a value of an undoped material.

Furthermore, this study the difference in the lifetime of doped state of polypyrrole obtained from different methods, the following experiments were carried out. Polypyrrole films prepared by AC plasma polymerization at 30, 60, and 90 minute of 800 V were doped by placing them in a sealed container containing iodine crystals for 24 hours (*ex situ*). After the doping process, the films were taken out of the chamber and were let stand in ambient atmosphere. Subsequently, the conductivity of these materials was determined by a two-point probe method. Conductivity of the films was measured at intervals of time to determine the decreasing rate of conductivity. Later, *ex situ* iodine-doped plasm-polymerized polypyrrole films were measured the conductivity around 6.8×10^{-7} to 32.0×10^{-7} S/cm which are higher than *in situ* iodine-doped plasma-polymerized polypyrrole films (8.4×10^{-7} to 16.6×10^{-7} S/cm). As mentioned previously, this doping method which iodine were covered on the polymer surface cause for iodine easily diffuse to the polymer. And this doping method has doping degree higher close to the surface than at the inner layer film which results in unstable doping. Thus, these films were also measured the electrical conductivity of the post-doping for various periods of time is depicted in **Figure 4.20** in order to compare the conductivity with *in situ* doping. It was found that during the post-doping period, conductivity of the doped materials rapidly decreased that of undoped plasma-polymerized polypyrrole in approximately 5 hours (300 minute).

The fast decay is not surprising since iodine could only be adsorbed mostly on the surface of the polypyrrole films. This physical interaction is rather weak. As a result diffusion of the adsorbed iodine can occur over time.

For the conductivity of plasma polypyrrole after overnight exposure to iodine vapor doping decreases rapidly, until the conductivity are approximate undoped plasma-polyermerized polypyrrole films. It is probably due to the diffusion of absorbed iodine from the surface films. The *in situ* doping has the higher stability iodine-doped as shown in **Figure 4.20**. Apparently, the films lost their conductivity in a longer period of time compared to the results obtained from traditional doping method. Therefore, the *in situ* doping had presumably evenly distributed iodine dopant all over the entire bulk of the films. It can be proved that *in situ* doping provides the increased conductivity and high stability for a long time.

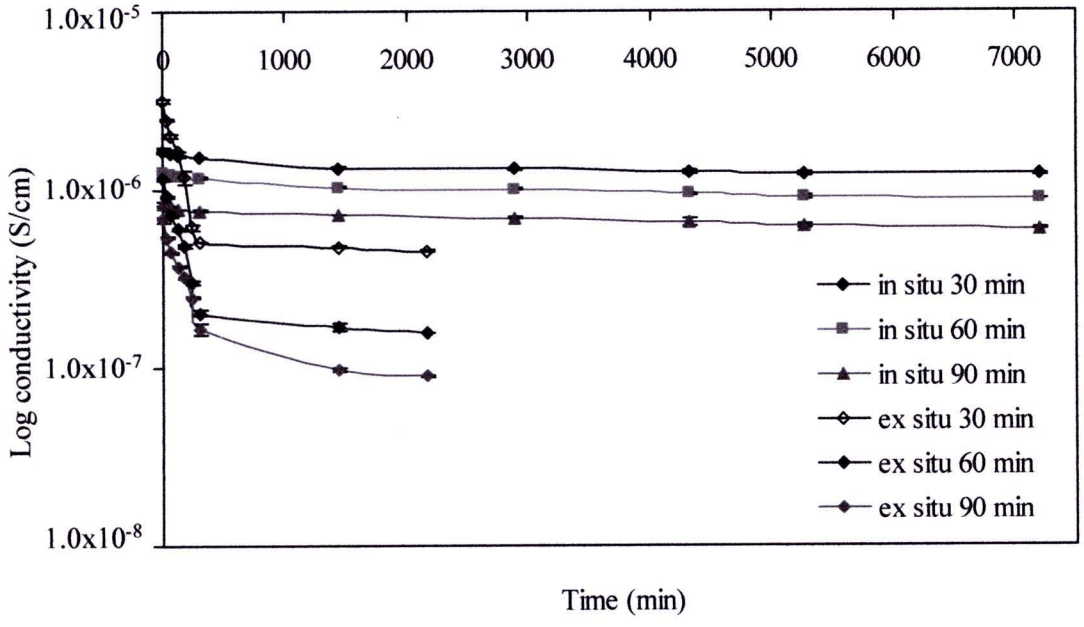

Figure 4.20 The conductivity of *in situ* iodine-doped plasma-polymerized polypyrrole and *ex situ* iodine-doped plasma-polymerized polypyrrole at various reaction times for 800 V as a function of exposure times.

Results presented thus far in this thesis have shown that AC plasma polymerization process can be an efficient method for fabricating conducting polymer films. Future work may include optimization of reaction conditions, testing of other

possible substances as dopants, modification of dopant introduction into the films, as well as finding good conditions to maintain conjugating system in the materials.